Molecular Biology of the Cell
Vol. 16, 2947–2959, June 2005

The PCH Family Member MAYP/PSTPIP2 Directly Regulates F-Actin Bundling and Enhances Filopodia Formation and Motility in Macrophages[D] [V]

Violeta Chitu,* Fiona J. Pixley,* Frank Macaluso,[†‡] Daniel R. Larson,[†] John Condeelis,[†‡] Yee-Guide Yeung,* and E. Richard Stanley*

Departments of *Developmental and Molecular Biology and [†]Anatomy and Structural Biology; and [‡]Analytical Imaging Facility, Albert Einstein College of Medicine, Bronx, NY 10461

Submitted October 21, 2004; Revised March 2, 2005; Accepted March 15, 2005
Monitoring Editor: David Drubin

***M*acrophage *a*ctin-associated t*y*rosine *p*hosphorylated protein (MAYP) belongs to the Pombe Cdc15 homology (PCH) family of proteins involved in the regulation of actin-based functions including cell adhesion and motility. In mouse macrophages, MAYP is tyrosine phosphorylated after activation of the colony-stimulating factor-1 receptor (CSF-1R), which also induces actin reorganization, membrane ruffling, cell spreading, polarization, and migration. Because MAYP associates with F-actin, we investigated the function of MAYP in regulating actin organization in macrophages. Overexpression of MAYP decreased CSF-1–induced membrane ruffling and increased filopodia formation, motility and CSF-1-mediated chemotaxis. The opposite phenotype was observed with reduced expression of MAYP, indicating that MAYP is a negative regulator of CSF-1–induced membrane ruffling and positively regulates formation of filopodia and directional migration. Overexpression of MAYP led to a reduction in total macrophage F-actin content but was associated with increased actin bundling. Consistent with this, purified MAYP bundled F-actin and regulated its turnover in vitro. In addition, MAYP colocalized with cortical and filopodial F-actin in vivo. Because filopodia are postulated to increase directional motility by acting as environmental sensors, the MAYP-stimulated increase in directional movement may be at least partly explained by enhancement of filopodia formation.**

INTRODUCTION

Macrophages are important in the innate and adaptive immune response (Stoy, 2001), tissue and organ development (Pollard and Stanley, 1996), angiogenesis (Lewis *et al.*, 1995) and tumor cell metastasis (Coussens and Werb, 2001; Lin *et al.*, 2001). Central to their role in these biological processes is their capacity to migrate, to populate various tissues, and to phagocytose. Migration, invasion and phagocytosis are actin-based cellular events. CSF-1 is the primary growth factor regulating the development and maintenance of tissue macrophages (Stanley *et al.*, 1978; Tushinski *et al.*, 1982; Cecchini *et al.*, 1994; Pixley and Stanley, 2004). CSF-1 also stimulates rapid reorganization of the actin cytoskeleton and is chemotactic both in vitro (Boocock *et al.*, 1989; Webb *et al.*, 1996; Pixley *et al.*, 2001) and in vivo (Wyckoff *et al.*, 2004). The effects of CSF-1 are mediated via the CSF-1 receptor tyrosine kinase (Sherr *et al.*, 1985), which, in response to CSF-1, mediates tyrosine phosphorylation of many cellular proteins (Yeung and Stanley, 2003), including MAYP (Yeung *et al.*, 1998b). MAYP, also known as proline-serine-threonine-phosphatase-interacting protein 2 (PSTPIP2; Wu *et al.*, 1998a), is the major F-actin–associated, tyrosine-phosphorylated protein in the cytosolic fraction of CSF-1–stimulated macrophages (Yeung *et al.*, 1998a, 1998b). It belongs to the PCH family of proteins whose members are involved in the regulation of actin-based functions such as cytokinesis, endocytosis, cell adhesion, and motility (Lippincott and Li, 2000). The PCH family members share a similar domain organization, including an amino-terminal Fes-CIP4 Homology domain (FCH) followed by a coiled-coil domain, proline-glutamic acid-serine-threonine–rich (PEST) sequences, and a Src homology domain 3 (SH3; Lippincott and Li, 2000). MAYP contains an amino-terminal FCH domain (amino acids 13–98) followed by a potential coiled-coil domain (amino acids 93–121) and a conserved basic and acidic residue–rich region (amino acids 99–160), but lacks the PEST motifs and the SH3 domain (Yeung *et al.*, 1998b).

Overexpression studies have shown that different members of the PCH family expressed in mammalian cells regulate various aspects of actin organization to affect actin polymerization, membrane ruffling, formation of filopodia,

This article was published online ahead of print in *MBC in Press* (http://www.molbiolcell.org/cgi/doi/10.1091/mbc.E04–10–0914) on March 23, 2005.

[D] [V] The online version of this article contains supplemental material at *MBC Online* (http://www.molbiolcell.org).

Address correspondence to: E. Richard Stanley (rstanley@aecom.yu.edu).

Abbreviations used: AFU, arbitrary fluorescence units; CIP4, Cdc42-associated protein 4; CSF-1, colony-stimulating factor-1; CSF-1R, colony-stimulating factor-1 receptor; FCH, Fes-CIP4 homology domain; GFP, green fluorescent protein; IRES, internal ribosomal entry site; MAYP, macrophage actin-associated tyrosine-phosphorylated protein; MSCV, murine stem cell virus; NαMAYP-C, rabbit IgG anti-MAYP preabsorbed with nuclear extract; N-WASP, neural WASP; PEST, proline-glutamic acid-serine-threonine–rich; PSTPIP, proline serine threonine phosphatase–interacting protein; PCH, Pombe Cdc15 homology; RaIgG, preimmune rabbit immunoglobulin G; RPE, relative plating efficiency; SEM, scanning electron microscopy; SH3, Src homology domain 3; Syndapin, synaptic dynamin-associated protein; WASP, Wiskott-Aldrich syndrome protein.

cell adhesion, and motility. For example, overexpression of Cdc42-associated protein 4 (CIP4) decreased the number of stress fibers in Swiss 3T3 fibroblasts (Aspenström, 1997), whereas overexpression of rat synaptic, dynamin-associated protein I (Syndapin I) or Syndapin II, caused reorganization of cortical F-actin and formation of filopodia in HeLa cells (Qualmann and Kelly, 2000). In addition, hyperphosphorylation of PSTPIP1, a PCH family member closely related to MAYP, was associated with defects in focal adhesion disassembly, migration, and cytokinesis in fibroblasts (Angers-Loustau *et al.*, 1999).

The SH3 domain of many of these proteins seems to be crucial for their function, because it interacts with the Wiskott-Aldrich syndrome protein (WASP) or neural WASP (N-WASP), two activators of the Arp2/3 actin polymerization machinery (Lippincott and Li, 2000; Takenawa and Miki, 2001). The interaction between PSTPIP1 and WASP was reported to result in loss of WASP-induced actin bundling (Wu *et al.*, 1998b), whereas the interaction of Transducer of Cdc42-dependent actin assembly (Toca-1) with N-WASP promotes actin nucleation by activating the N-WASP-WIP/CR16 complex (Ho *et al.*, 2004). CIP4 interacts with WASP and microtubules, thereby facilitating the transport of WASP to sites of substrate adhesion in hematopoietic cells (Tian *et al.*, 2000). The interaction of Syndapins and of their mouse homologues, the protein kinase C and CK2 substrate in neurons (PACSINs) with N-WASP and with two other proteins implicated in vesicular traffic, synaptojanin and dynamin, reflects an important functional link between vesicular trafficking and actin dynamics (Modregger *et al.*, 2000; Qualmann and Kelly, 2000).

On the basis of these data, we hypothesized that MAYP could regulate the organization of the actin cytoskeleton downstream of CSF-1R activation in macrophages. Because MAYP lacks the C-terminal SH3 domain and is therefore not likely to interact with WASP, it was of interest to investigate its function and mechanism of action in macrophages. In the present article, we demonstrate that MAYP is an actin-bundling protein that controls the organization of the actin cytoskeleton and the morphology and motility of macrophages.

MATERIALS AND METHODS

Reagents and Chemicals

The following antibodies were used: mouse anti-actin (Chemicon International, Temecula, CA), mouse anti-phosphotyrosine PY20 (Transduction Laboratories, Lexington, KY). FITC-coupled anti-mouse IgG (Jackson ImmunoResearch Laboratories, West Grove, CA), Alexa 647–coupled anti-rabbit IgG, rhodamine-labeled phalloidin and TRITC-coupled anti-mouse IgG were from Molecular Probes (Eugene, OR). Unless stated otherwise, all other reagents and chemicals were purchased from Sigma (St. Louis, MO).

Cell Culture and Stimulation

Macrophages of the BAC1.2F5 cell line (Morgan *et al.*, 1987) were maintained in growth medium comprising α-MEM (Life Technologies, Grand Island, NY) supplemented with 10% (vol/vol) newborn calf serum, 1.32 nM CSF-1 (a gift from Chiron, Emeryville, CA), 2 mM L-glutamine, 0.15 mM L-asparagine, 15 nM β-mercaptoethanol, 77.5 U/ml streptomycin, and 25 U/ml penicillin. Cells were grown at 37°C in 100-mm tissue culture dishes (Becton Dickinson, San Diego, CA) in 5% CO_2 until 80% confluent. The cell monolayers were incubated for a further 18 h in CSF-1–free medium to allow for CSF-1 receptor up-regulation and then incubated with 13.2 nM CSF-1 at 37°C for the indicated times. Stimulation was arrested by washing the cells with ice-cold phosphate-buffered saline (PBS) and subcellular fractionation was performed as previously described (Yeung *et al.*, 1992).

MAYP Immunoprecipitation and Analysis of Associated Proteins

Antigen-immunoaffinity–purified α-MAYP-C antibody was covalently coupled to Affigel beads (Bio-Rad, Hercules, CA) at 2 mg IgG/ml packed beads. For MAYP immunoprecipitation, cytosolic extracts from CSF-1–stimulated or nonstimulated BAC1.2F5 cells containing 3 mg of total protein were mixed with antibody-coupled beads (25 μl packed beads/sample) and incubated overnight at 4°C. The immunoprecipitates were washed five times with washing/binding buffer (10 mM Tris HCl, pH 7.0, 5 μM $ZnCl_2$, 50 mM NaCl, 30 mM $Na_4P_2O_4$, 50 mM NaF, 0.5 mM Na_3VO_4, 0.5% Nonidet P- 40 [NP-40], 0.5 mM benzamidine). MAYP and coimmunoprecipitated proteins were eluted using 12.5 μl of 3× concentrated Laemmli sample buffer and the supernatant was separated by 5–15% gradient SDS-PAGE (acrylamide-bisacrylamide 30:8). Proteins were transferred to 0.2-μm polyvinylidene difluoride membrane (Schleicher & Schuell, Keene, NH) using a transfer buffer containing 25 mM Tris, 192 mM glycine, 0.01% SDS, and 5% methanol. Membranes were blocked using Tris-buffered saline containing 1% bovine serum albumin and 3% teleostean gelatin for 1 h at 37°C and subsequently probed with various antibodies. Immunoreactive proteins were visualized by enhanced chemiluminescence (ECL, Amersham, Piscataway, NJ).

Immunofluorescence Staining

Cell fixation and immunofluorescence staining were carried out as previously described (Pixley *et al.*, 2001). Briefly, cells were seeded onto fibronectin-coated coverslips (Becton Dickinson, Bedford, MA) in six-well culture plates. At 30–50% confluence, cells were fixed, permeabilized, and stained as described (Pixley *et al.*, 2001). After washing, coverslips were dried and mounted in Prolong Antifade (Molecular Probes) and all samples were examined under an Olympus inverted microscope (Melville, NY) with images recorded using a Photometrics CH cooled charge coupled device (CCD) camera using IP lab spectrum software (VayTek, Fairfield, IA). For the fluorescence quantification, images were captured below the saturation level of the camera. The F-actin content of the cells was quantitated by measuring the pixel fluorescence intensity using the ImageJ software (DesMarais *et al.*, 2002).

Detection of Cellular MAYP

To study the function and cellular location of MAYP, an anti-MAYP peptide antibody (Yeung *et al.*, 1998b) to amino acids 292–309 of MAYP (α-MAYP-C) was raised in rabbit. The specificity of α-MAYP-C was analyzed by Western blotting of BAC1.2F5 macrophage fractions (Supplementary Figure S1A). The antibody reacted with MAYP in the cytosol of BAC1.2F5 cells (Supplementary Figure S1A, lane Cy). In longer exposures, small amounts of MAYP were also found in the NP-40–soluble membrane and cytoskeletal fractions but not in the nuclear fraction (unpublished data and see Figure 4 of Yeung *et al.*, 1998b). However, cross-reactivity with a 63-kDa protein was observed in the NP-40–soluble membrane cytoskeletal and nuclear fractions (Supplementary Figure S1A, lanes M, Csk, and N). Immunofluorescence staining with α-MAYP-C (10 μg/ml) resulted in diffuse cytoplasmic and nucleolar staining (Supplementary Figure S1C1). To eliminate the cross-reactivity with the 63-kDa protein, the α-MAYP-C was preabsorbed for 1 h at 20°C with NP-40–soluble nuclear extract (Nα-MAYP-C). Preabsorption with nuclear extract eliminated both the cross-reactivity with p63 (Supplementary Figure S1B) and the nucleolar staining (Figure S1C2). Preincubation of Nα-MAYP-C with 250-fold molar excess of the peptide antigen for 2 h at 20°C completely blocked the Nα-MAYP-C staining (Supplementary Figure S1C3).

Sense and Antisense pMSCV-MAYP-IRES-GFP Constructs

To investigate the function of MAYP, a Murine Stem Cell Virus (MSCV)-derived bicistronic retroviral vector, pMSCV-IRES-GFP (a gift from Dr. R. G. Hawley, University of Toronto, Canada), was used to alter the level of expression of MAYP in macrophages. In this vector, the internal ribosome entry site (IRES) allows simultaneous expression of a protein of interest and of the green fluorescent protein (GFP). Using PCR, *Eco*RI sites and a single copy of the myc tag were attached in frame to the 5′ end of the cDNA of MAYP (NCBI Accession no. Y18101). The resulting myc-tagged constructs were ligated in sense or antisense orientation into the *Eco*RI site of the pMSCV-IRES-GFP retroviral expression vector (Persons *et al.*, 1999) between the long terminal repeat (LTR) retroviral promoter and the IRES. The final constructs were checked by DNA sequencing and used to increase or lower the level of expression of MAYP in BAC1.2F5 macrophages, respectively.

Transfection, Retroviral Infection, and Stable Cell Line Selection

The pMSCV-MAYP-IRES-GFP constructs and the helper plasmid ψ2 containing the packaging signal (Muller *et al.*, 1991) were cotransfected into 293T cells, using Lipofectamine (Invitrogen, Carlsbad, CA). The retroviral supernatants were harvested 48 h after transfection and filtered through a 0.45-μm filter. BAC1.2F5 macrophages in 100-mm tissue culture dishes were incubated with fresh retroviral supernatants (10 ml/dish) in the presence of 1.32 nM CSF-1 and 4 μg/ml polybrene for 24 h, cultured for 6 more days and subjected to fluorescence-activated cell sorting (FACS; FACSVantage SE; BD Biosciences, San Jose, CA) for GFP-positive cells. Sorted GFP-positive cells were used for single-cell cloning. The levels of MAYP expression in individual clones were analyzed by Western blot using MAYP-specific antibodies. The clones obtained were stable when maintained in culture for more than 2 mo.

Scanning Electron Microscopy and Quantification of CSF-1–induced Responses

Cells were grown on 22-mm circular glass coverslips in six-well cell culture plates to 50–70% confluence and then incubated for 16–18 h in CSF-1–free medium to induce CSF-1R up-regulation. The up-regulated cells were stimulated with CSF-1 for the indicated times, the coverslips were rinsed with PBS, and the cells were fixed quickly with osmium tetroxide followed by staining with gold-palladium as described (Pixley *et al.*, 2001). The presence of filopodia and membrane ruffling was examined using a JEOL JSM6400 scanning electron microscope (Peabody, MA) using an accelerating voltage of 5 kV. All measurements necessary to quantify the CSF-1–induced responses were done using ImageJ 1.33k software (W. S. Rasband, ImageJ, National Institutes of Health, Bethesda, MD, http://rsb.info.nih.gov/ij/, 1997–2004). Cell spreading was estimated by manually tracing the cell perimeter and measuring the cell footprint area (C; Supplementary Figure S2). Ruffling was estimated by manually tracing the perimeter of the ruffles and measuring the area (ruffling area, R; Supplementary Figure S2). The percent ruffling for each cell was obtained by dividing the ruffling area by the sum of ruffling area and cell area $((R \times 100)/(R + C))$. The number and length of filamentous protrusions were determined by counting and manual tracing, respectively.

Time-lapse Video Microscopy

Cells were plated on MatTek cell culture dishes (Ashland, MA) at low density and cultured for 2 d before the experiment. The plates were placed on the stage of an Olympus IX70 inverted microscope equipped with a humidified, 5% CO2-containing, 37°C temperature-controlled chamber. Phase-contrast images of five different fields were acquired at 60-s intervals using a Cooke Sensicam QE cooled CCD camera (Auburn Hills, MI) with Scanalytics IPLab software (Fairfax, VA) running on a Dell PC (Round Rock, TX). Sequences were assembled and quantified using ImageJ 1.33k software. Filopodia formation was assessed by visual inspection of the time-lapse movies.

Immunogold Labeling, Rotary Shadowing, and Transmission Electron Microscopy

Cells were grown on glass coverslips, fixed, immunolabeled, and processed for rotary shadowing as described (Bailly *et al.*, 1999). The samples were observed using a JEOL 100CX transmission electron microscope at 100 kV. The immunolabeling of MAYP was carried out as described (Bailly *et al.*, 1998) using either rabbit anti-MAYP or 9E10 mouse anti-myc antibodies (Covance, Grand Rapids, MI) followed by 10-nm gold-coupled goat anti-rabbit IgG or 6-nm gold-coupled goat anti-mouse IgG (EMS, Hatfield, PA), respectively.

Motility and Chemotaxis Assays

Macrophage directional movement was evaluated as described (Pixley *et al.*, 2001) using a wound-healing assay. CSF-1–stimulated chemotactic migration was determined using BD BioCoat FluoroBlok Fibronectin Cell Culture Inserts (BD Labware, Franklin Lakes, NJ) and calcein red-orange AM (Molecular Probes) staining as described (Rust *et al.*, 2000). Briefly, cells were rinsed with CSF-1–free medium, harvested using a plastic cell lifter, centrifuged, and resuspended at 10^6 cells/ml in CSF-1–free medium. A volume of 200-μl cell suspension was added to the FlouroBlok inserts, and the inserts were introduced in the wells of a 24-well cell culture plate each containing 700 μl of α-MEM and 1.32 nM CSF-1. Cells were then incubated for 16 h at 37°C to allow for migration. Thirty minutes before the end of the assay, the medium in the lower chamber was adjusted to 10 μM Calcein red-orange AM (Molecular Probes), and cells were further incubated for 30 min at 37°C. The inserts were then washed four times with PBS, and cell migration was evaluated by reading the fluorescence of Calcein red–labeled cells that had migrated on the bottom of the FluoroBlok insert using a Polar Star Optimas microplate reader (Media Cybernetics, Silver Spring, MD; Rust *et al.*, 2000). For each assay, samples were run in triplicate.

In contrast to the wound healing assay, which measures the movement of already adherent cells, the chemotaxis assay requires replating of the cells and the results are influenced by the plating efficiency. Macrophages underexpressing MAYP have a higher efficiency of plating than cells expressing normal or higher levels of MAYP (unpublished data). To evaluate the plating efficiency, 200 μl of the same cell suspension used for the chemotaxis assay was added to 35-mm cell culture dishes containing 2 ml of α-MEM supplemented with 1.32 nM CSF-1 and the cells were allowed to adhere for 16 h at 37°C. Phase-contrast pictures of three different fields were taken, and the average number of adherent cells was used to determine the relative plating efficiency (RPE). The fluorescence readings, expressed in arbitrary fluorescence units (AFU), were then normalized to the relative plating efficiency for each clone (AFU/RPE).

Purification of myc-MAYP and EF-1α

Myc-tagged MAYP (mycMAYP) was affinity-purified from the NP-40–soluble lysate of cycling BAC1.2F5 cells overexpressing MAYP by affinity chromatography using the anti-myc monoclonal antibody 9E10 cross-linked to protein G agarose beads (Zymed, San Francisco, CA) and eluted under nondenaturing conditions using 10 mM myc peptide. EF-1α was purified from *Dictyostelium discoideum* as described (Demma *et al.*, 1990).

Actin-bundling Assays

Purified mycMAYP was concentrated by ultrafiltration through a 10-kDa cutoff Amicon Ultra-4 centrifugal filter device (Millipore, Bedford, MA), diluted in sedimentation buffer (Edmonds *et al.*, 1996) and similarly diluted and concentrated again twice more to exchange the buffer. The actin-bundling assays were performed as described (Demma *et al.*, 1990) using 3 μM actin and either purified mycMAYP or purified EF-1α (1 μM) in a final volume of 30 μl. The extent of bundling was evaluated by electron microscopic analysis of uranyl acetate–stained samples (Demma *et al.*, 1990). To determine the distribution of MAYP or EF-1α on the in vitro–polymerized bundles, aliquots of each sample (5 μl) were adsorbed on Formvar and carbon-coated copper grids, stained with anti-MAYP or anti-EF-1α antibodies and the appropriate gold-coupled secondary antibodies as described (Bailly *et al.*, 1999), washed quickly with 2 mM $MgCl_2$, and negatively stained.

In Vitro Actin Polymerization/Depolymerization

A G-actin mixture was prepared as a mixture of ~90% unlabeled rabbit actin and 10% pyrene-labeled rabbit actin in buffer A (2 mM Tris, 0.2 mM $CaCl_2$, 0.2 mM ATP, 0.02% NaN_3, 0.5 mM dithiothreitol [DTT], pH 8.0). Polymerization was initiated by addition to the G-actin solution of an equal volume of 2× polymerization buffer KMg50 (20 mM imidazole, 4 mM $MgCl_2$, 100 mM KCl, 2 mM ATP, 2 mM EGTA, 2 mM DTT, pH 7.0). Depolymerization was initiated by diluting the resulting F-actin solution into depolymerization buffer (20 mM Tris, 2 mM $MgCl_2$, 50 mM KCl, 5 mM EGTA, 1 mM ATP, 1 mM DTT, pH 7.6). Fluorescence measurements were done on a FluoStar Optima 96-well plate reader (BMG Labtech, Durham, NC) with excitation wavelength, 360 nm; and emission wavelength, 405 nm.

RESULTS

MAYP Inhibits Membrane Ruffling and Stimulates Both Filopodia Formation and Cell Polarization in Macrophages

To determine the function of MAYP in macrophages, BAC1.2F5 macrophages were retrovirally infected with the MSCV-mycMAYP-IRES-GFP vector, encoding amino-terminally myc-tagged full-length MAYP, the MSCV-ASMAYP-IRES-GFP encoding antisense MAYP mRNA, or the MSCV-IRES-GFP vector alone. Cells from three separate infections were cloned and the level of MAYP expression in 22 empty vector, 16 MAYP antisense, and 25 MAYP-overexpressing clones was determined by Western blotting with Nα-MAYP-C antibody. In addition, the morphology of cultured cells of each clone was examined by phase-contrast microscopy. Among these 63 clones, a gradation of morphological characteristics was observed that correlated with the level of expression of MAYP. The morphologies of vector-infected cells and uninfected cells were indistinguishable (unpublished data). Clones stably expressing high (MAYP OE C2), moderately high (MAYP OE B9), moderately low (MAYP AS C3), and low levels (MAYP AS C8) of MAYP were chosen for further characterization.

Increased expression of MAYP was correlated with increased cell spreading and elongation (Figure 1A, two right panels). With reduced MAYP expression, the cells were star-shaped or circular and tended to be much less elongated (Figure 1A, two left panels) and under scanning electron microscopy, these macrophages displayed many large dorsal ruffles and few filopodia (Figure 1B, two left panels). In contrast, cells overexpressing MAYP displayed few dorsal ruffles and possessed numerous filopodia (Figure 1B, two right panels). Filopodia and retraction fibers are morphologically indistinguishable. Confirmation that the hair-like membrane protrusions were indeed filopodia and not retraction fibers was obtained by time-lapse videomicroscopy of cells expressing normal and altered levels of MAYP (see Supplementary Movies S1 of clone AS, 0.3×; S2 of clone V, 1×; and S3 of clone OE, 27×). From the time-lapse data we have estimated the rate of filopodia formation in cells grown

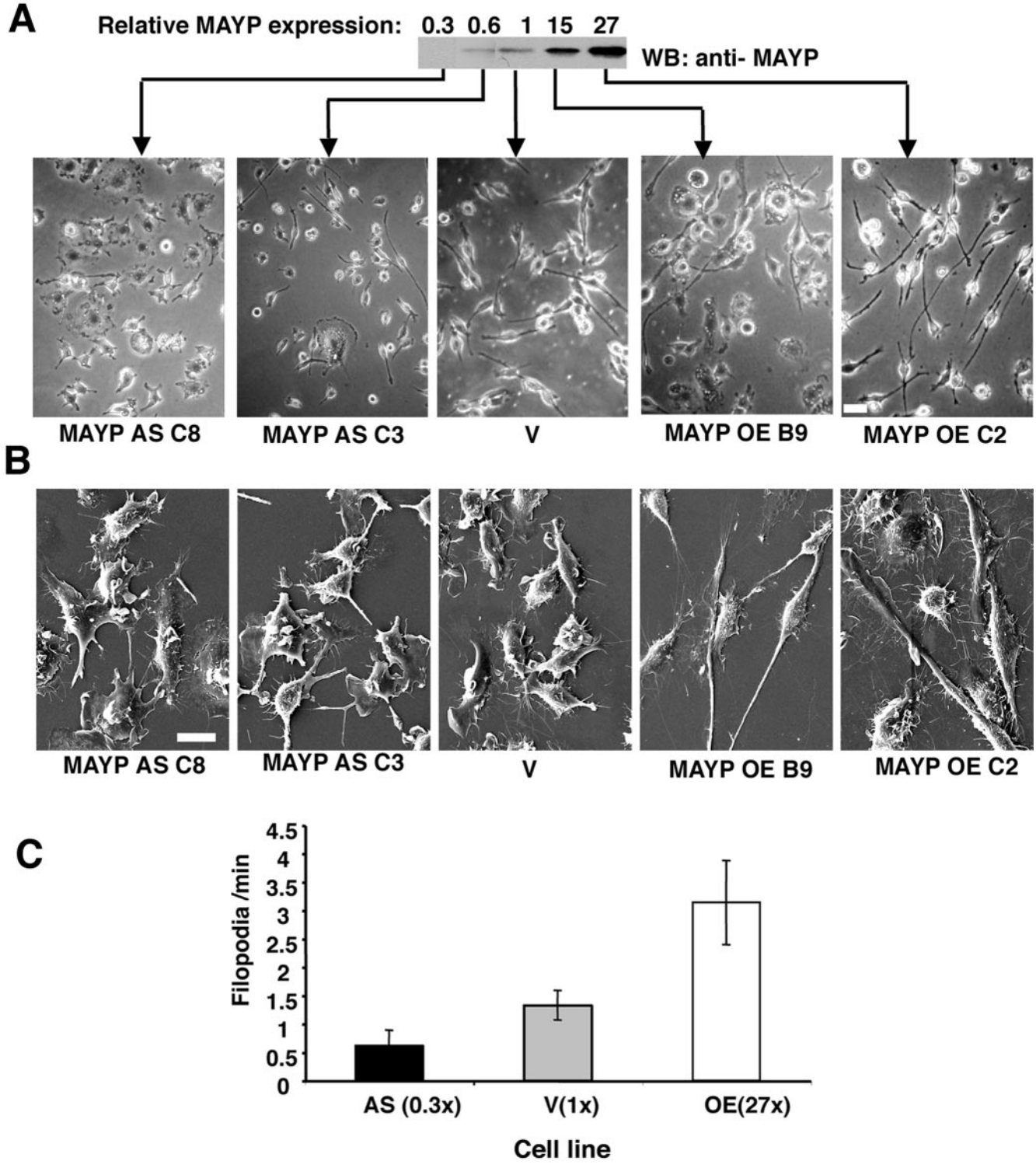

Figure 1. MAYP inhibits CSF-1–induced membrane ruffling and stimulates the formation of filopodia and cell elongation. (A) The morphology of retrovirally infected BAC1.2F5 macrophages expressing normal and altered levels of MAYP was examined using phase contrast microscopy of living cells. Cells were cultured in the presence of CSF-1. AS, antisense; V, empty vector; OE, overexpression. Top, anti-MAYP Western blot of SDS lysates of clones expressing normal and altered levels of MAYP. The quantification of the chemiluminescent signal was carried out on scanned films using Image Quant software (individual lanes from original film resulting from test of 11 different clones). (B) Morphology of these macrophages examined by scanning electron microscopy. (C) Dynamics of filopodia formation in macrophages expressing normal and altered levels of MAYP. The rate of filopodia formation in living cells was determined from time-lapse movies of clones expressing normal and altered levels of MAYP (AS MAYP, 0.3×; V, 1×; and MAYP OE, 27×) by counting the number of new filopodia formed in each frame. On average, 14 cells per clone were evaluated. Error bars, represent the SD of the mean. All differences between cell lines are statistically significant ($p < 0.00001$, Student's t test). Scale bars, 20 μm in A; 10 μm in B.

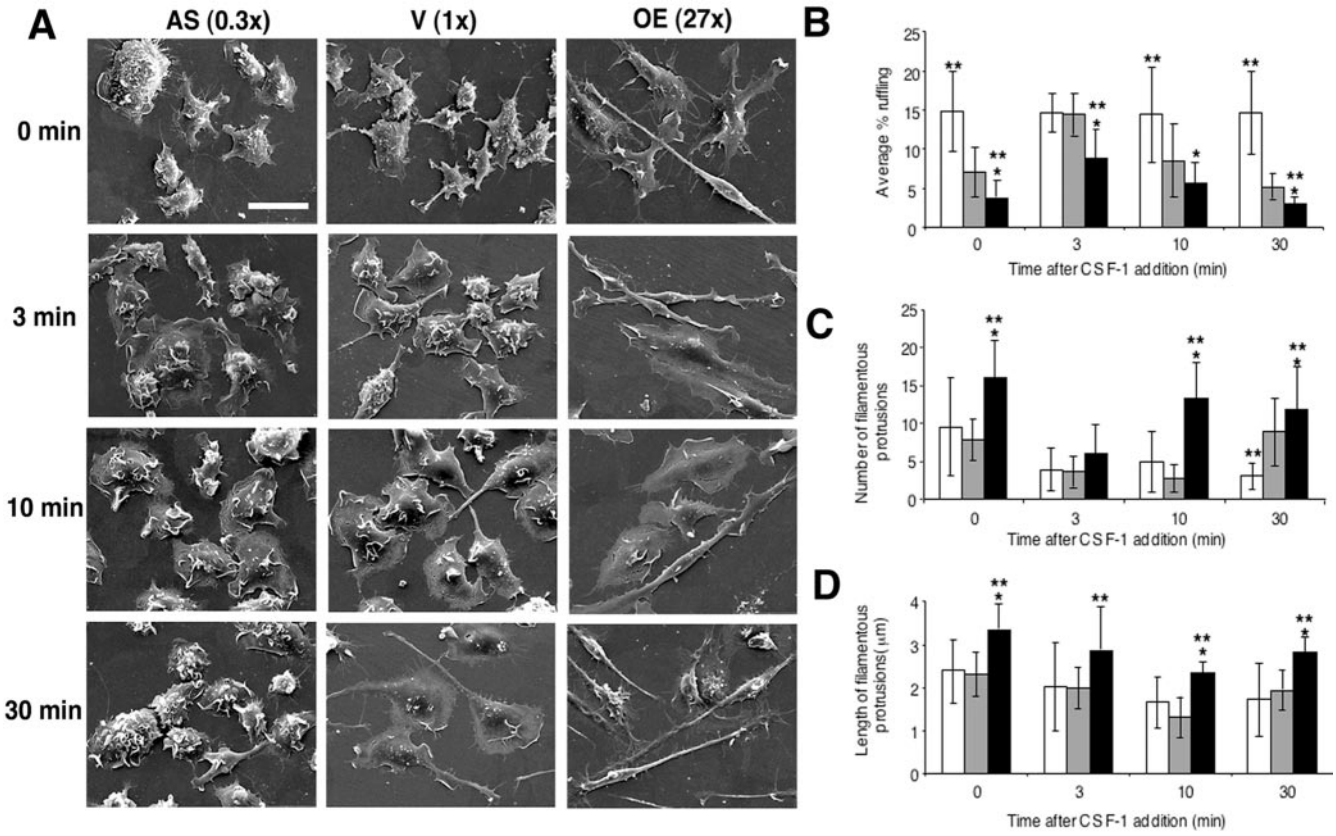

Figure 2. CSF-1 morphological responses are regulated by MAYP. (A) Kinetics of CSF-1–stimulated responses in macrophages expressing normal and altered levels of MAYP. Macrophages were deprived of CSF-1 for 18 h and then stimulated with CSF-1 for the indicated times. CSF-1–induced morphological changes were evaluated by SEM (1500× magnification). The level of MAYP expression relative to endogenous MAYP is shown in brackets. Scale bar, 20 μm. (B–D) Quantitative analysis of the kinetics of CSF-1–stimulated membrane ruffling (B, ~17 cells/clone/time point) and the number (C) and length (D) of filamentous protrusions (~116 filamentous protrusions/clone/time point); open bars, antisense; gray bars, vector; black bars, overexpression. Means ± SD; *different from antisense; **different from vector ($p < 0.05$).

in the continuous presence of CSF-1 (Figure 1C). Consistent with the scanning electron microscopy data obtained with fixed cells, live cells overexpressing MAYP have been found to generate filopodia at a rate 2.4 times higher than control cells and 5 times higher than cells with reduced MAYP expression.

CSF-1–stimulated Responses Are Regulated by MAYP

Addition of CSF-1 to quiescent BAC1.2F5 macrophages induces the reorganization of the actin cytoskeleton, membrane ruffling, cell spreading, and polarization (Boocock *et al.*, 1989). We therefore investigated how the level of MAYP expression affected the response of macrophages to CSF-1 stimulation.

In the absence of CSF-1, BAC1.2F5 macrophages expressing normal or reduced levels of MAYP were rounded-up, apolar, and displayed numerous small dorsal ruffles and few filamentous protrusions (Figure 2A). Addition of CSF-1 to vector-infected cells for 3–10 min stimulated the formation of large dorsal ruffles (Figure 2, A and B) and resulted in cell spreading and in a reduction of the number of filamentous protrusions (Figure 2, A and C). After 30 min of stimulation, the ruffling response was attenuated and the cells adopted an elongated morphology with renewed filamentous protrusions (Figure 2, A–C). In cells expressing reduced levels of MAYP, the spreading response was also observed after the addition of CSF-1 but the ruffling was more intense at all time points and was not further stimulated after the addition of CSF-1 (Figure 2, A and B). Furthermore, there was no obvious CSF-1–induced cell polarization or formation of filamentous protrusions in macrophages expressing reduced levels of MAYP (Figure 2, A and C). In contrast, macrophages overexpressing MAYP exhibited an elongated morphology even in the absence of CSF-1, ruffled less, and possessed more numerous and longer filamentous protrusions (Figure 2, A–D). Although the addition of CSF-1 to these cells for 3–10 min resulted in cell spreading and a transient disappearance of filamentous protrusions (Figure 2, A and C), the CSF-1–stimulated ruffling was attenuated (Figure 2, A and B). Cell spreading regressed 30 min after CSF-1 addition, by which time numerous long filamentous protrusions were again evident (Figure 2, A, C, and D). There was no significant difference between clones over- and underexpressing MAYP in the kinetics or magnitude of the CSF-1–induced spreading response (unpublished data). Thus, MAYP stimulates the formation of filamentous protrusions and macrophage elongation and inhibits membrane ruffling.

CSF-1 Stimulates Tyrosine Phosphorylation of MAYP and Down-regulates Its Association with Membrane Ruffles

The morphology of macrophages expressing altered levels of MAYP and the alterations in their response to CSF-1

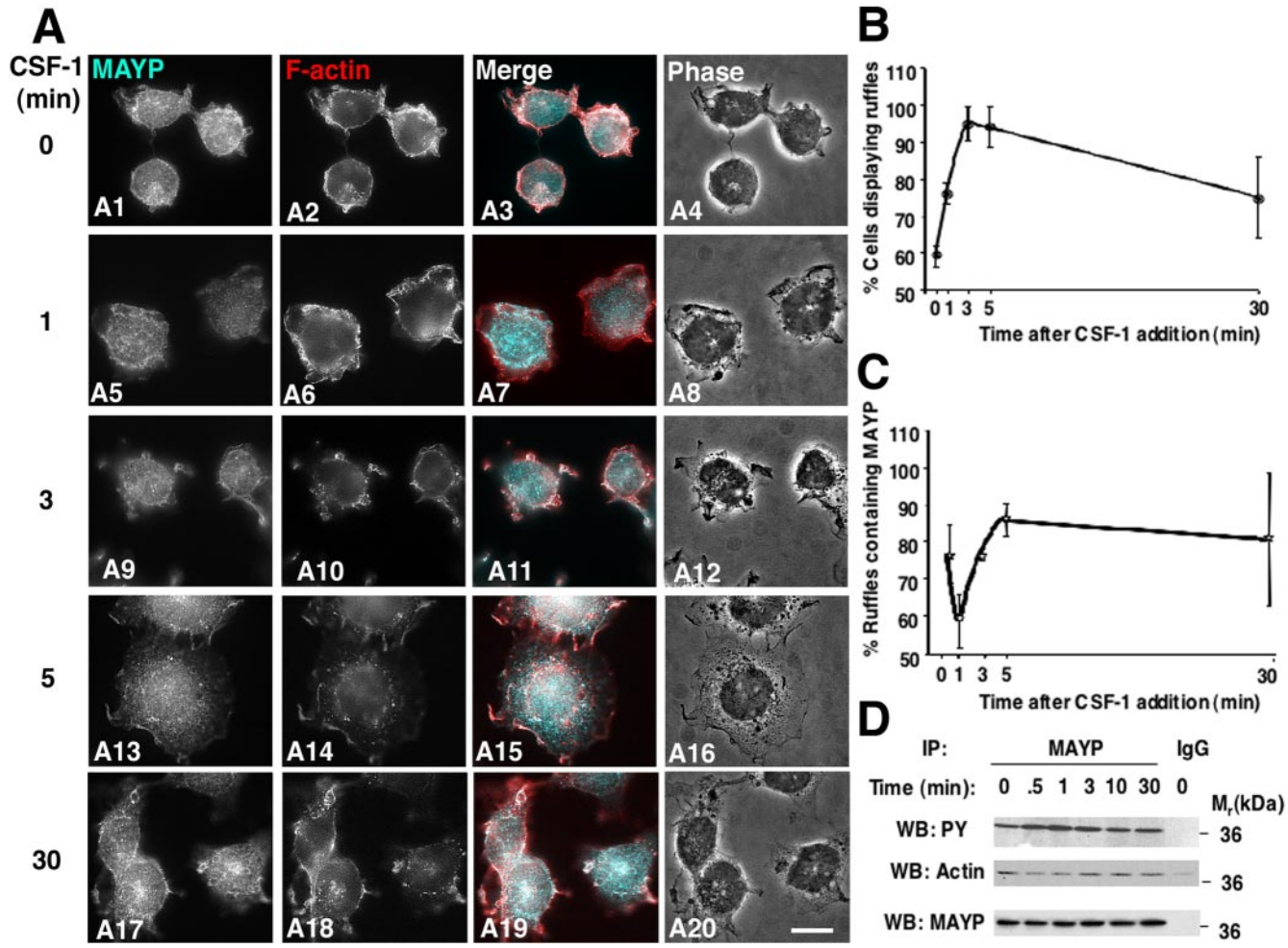

Figure 3. Colocalization of MAYP with ruffles is inversely related to MAYP tyrosine phosphorylation during CSF-1 stimulation of membrane ruffling. (A) Kinetics of association of endogenous MAYP with membrane ruffles in CSF-1–stimulated macrophages. Macrophages were deprived of CSF-1 for 18 h and then stimulated with CSF-1 for the indicated times. The white pixels in the merged panels indicate colocalization of MAYP (aqua) and F-actin (red). Scale bar, 10 μm. (B) Quantification of the extent of ruffling. (C) Quantification of MAYP association with the ruffles. (D) Time course of MAYP-stimulated tyrosine phosphorylation and association with cytosolic F-actin. Immunoprecipitates of MAYP from the cytosolic fraction of macrophages were subjected to SDS-PAGE and Western blotted with the indicated antibodies. Previous studies indicate that cytosolic MAYP binds F-actin not G-actin (Yeung *et al.*, 1998a, 1998b; Yeung and Stanley, 2003 and unpublished data).

indicate that MAYP inhibits CSF-1–induced membrane ruffling. We therefore examined the colocalization of MAYP with F-actin in CSF-1–stimulated BAC1.2F5 macrophages. Quiescent macrophages were rounded (Figure 3, A1–A4), with membrane ruffles displaying both F-actin and MAYP (Figure 3, A1–A3). Within 1 min of stimulation, the cells began to spread forming prominent F-actin–containing lamellipodia and ruffles (Figure 3, A5–A8). The colocalization of MAYP and F-actin in the ruffles transiently decreased at 1 min (Figure 3, A5–A7) due to a decrease in the number of ruffles containing MAYP (Figure 3C). Cell spreading and ruffling peaked at 3–5 min (Figure 3B) as did the intensity of MAYP staining in the ruffles (Figure 3, A9–A16). During this interval MAYP colocalized with F-actin in more than 80% of the ruffles (Figure 3, A11, A15, and C). By 30 min, the extent of membrane ruffling decreased (Figure 3, A20 and B) but the colocalization of MAYP with actin continued in the remaining ruffles (Figure 3, A17–A20 and C). Interestingly, the kinetics of MAYP tyrosine phosphorylation was inversely correlated with both its colocalization with F-actin in ruffles and its association with F-actin (Figure 3, C and D). These data are consistent with a role for MAYP in inhibiting cell ruffling downstream of CSF-1.

Macrophage Motility Increases with Increased MAYP Expression

The dramatic morphological alterations observed in macrophages expressing altered levels of MAYP suggested that MAYP could affect macrophage motility. We therefore studied the chemokinetic and chemotactic behavior of these cells. Macrophages overexpressing MAYP migrate more rapidly and macrophages expressing reduced levels of MAYP migrate more slowly than vector-infected macrophages in the wound-healing assay (Figure 4A). A rough estimate of the speed of migration was calculated by dividing the size of the gap scored in the confluent macrophage monolayer (~500 μm) by the time required for each clone to close the wound and was found to be ~0.35 μm/min for cells overexpressing MAYP, ~0.17 μm/min for the vector-infected

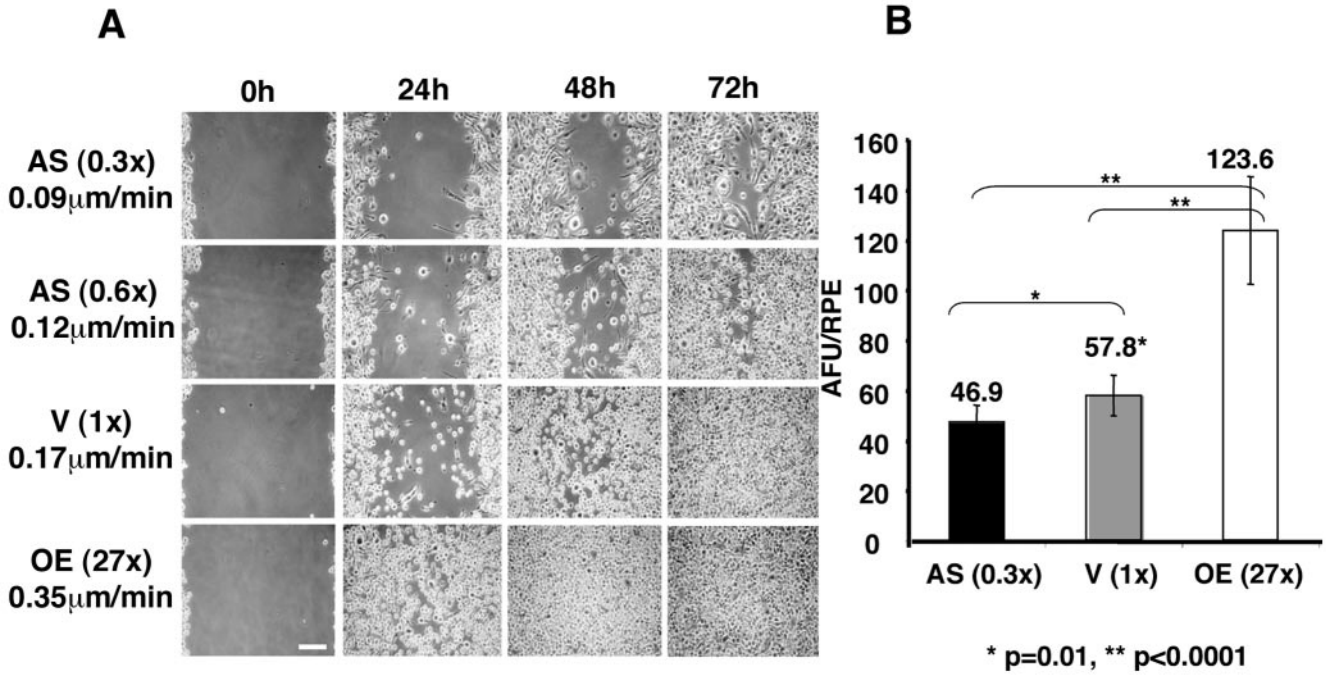

Figure 4. Macrophage motility and CSF-1–stimulated chemotaxis are proportional to the levels of expression of MAYP. (A). Directional migration in CSF-1 measured by a wound-healing assay. Cells were grown to confluence on tissue culture plastic, the monolayers scored to create a wound, and the cultures were fed daily with 1.32 nM CSF-1 medium and photographed live at 0, 24, 48, and 72 h. The calculated speed of migration (μm/min) of macrophages for each cell line is also shown. Scale bar, ~100 μm. (B) Chemotactic migration in a gradient of CSF-1. Cells (10^6/ml in CSF-1–free medium) were added to the FluoroBlok inserts and allowed to migrate for 16 h in a gradient of 0–1.32 nM CSF-1. Cells that migrated through the pores of the insert were stained with Calcein red-orange AM and detected using a Polar Star Optima microplate reader. The absorbance in fluorescence units (AFU) was normalized to the relative plating efficiency (RPE) as described in *Materials and Methods.* Results (±SD) are representative of three independent experiments that were carried out each using triplicate samples and the p values for comparison of migration were calculated by the Student's *t* test.

cells, and 0.12 and 0.09 μm/min for cells expressing 60 and 30% of the normal levels of MAYP, respectively.

Filopodia have been shown to be important for the chemotactic movement of macrophages (Allen *et al.*, 1998). We therefore determined the effects of altered expression of MAYP on CSF-1–stimulated macrophage migration. Compared with vector-infected cells, cells overexpressing MAYP exhibited increased chemotaxis, whereas the chemotactic migration of cells expressing reduced levels of MAYP was significantly reduced (Figure 4B).

Effect of MAYP on the Organization of the Macrophage Cytoskeleton

Because MAYP was previously shown to associate with F-actin (Yeung *et al.*, 1998b), we determined whether different levels of MAYP led to differences in the total amount of cellular F-actin and in the organization of the microfilament cytoskeleton. Decreased levels of total F-actin were found in macrophages overexpressing MAYP (Figure 5, A and B). In contrast, there was no difference in the total amount of actin present in each cell line (Figure 5C). Furthermore, ultrastructural analysis revealed that either overexpression, or reduction of MAYP levels, has dramatic effects on actin bundling (Figure 5D). In vector-infected cells, actin was organized into a dendritic network with an occasional radially oriented bundle (Figure 5D, arrow). In cells expressing reduced levels of MAYP, actin was organized into a loose dendritic network with very few bundles, whereas in cells overexpressing MAYP, there were many long, thick bundles of F-actin (Figure 5D). Indeed, in these cells the dendritic network consisted of thick bundles interconnected by thinner F-actin bundles throughout the lamellipodium, and single filaments were rarely detected.

MAYP Induces F-actin Bundling In Vitro

To determine if MAYP directly contributes to actin reorganization, we performed in vitro bundling assays where actin was polymerized in the presence or the absence of purified mycMAYP. The mycMAYP preparation was free of major contaminants as shown by SDS-PAGE and Western blotting or Coomassie blue staining (Figure 6A). When purified 3 μM G-actin was polymerized in vitro, the resulting F-actin was organized in long, straight individual filaments (Figure 6, B1 and B6). In the presence of mycMAYP, actin was polymerized and bundled into thick bundles interconnected by thinner bundles (Figure 6, B2 and B7), a structure similar to that observed in vivo in cells overexpressing MAYP (Figure 5D). Similar results were obtained with purified bacterially expressed GST-MAYP (Supplementary Figure S3). These experiments demonstrate that MAYP is capable of directly bundling F-actin in vitro.

We compared the structure of the actin bundles obtained with MAYP to bundles produced by another actin-bundling protein, EF1-α. In the presence of purified EF-1α the majority of actin was polymerized into thick, long, straight bundles with a highly organized, paracrystalline structure (Figure 6, B3 and B8). These contrast with the thinner, loosely packed, curved actin bundles observed upon copolymerization of MAYP with actin (Figure 6, B2 and B7). We also have examined the distribution of either MAYP or EF1-α on actin

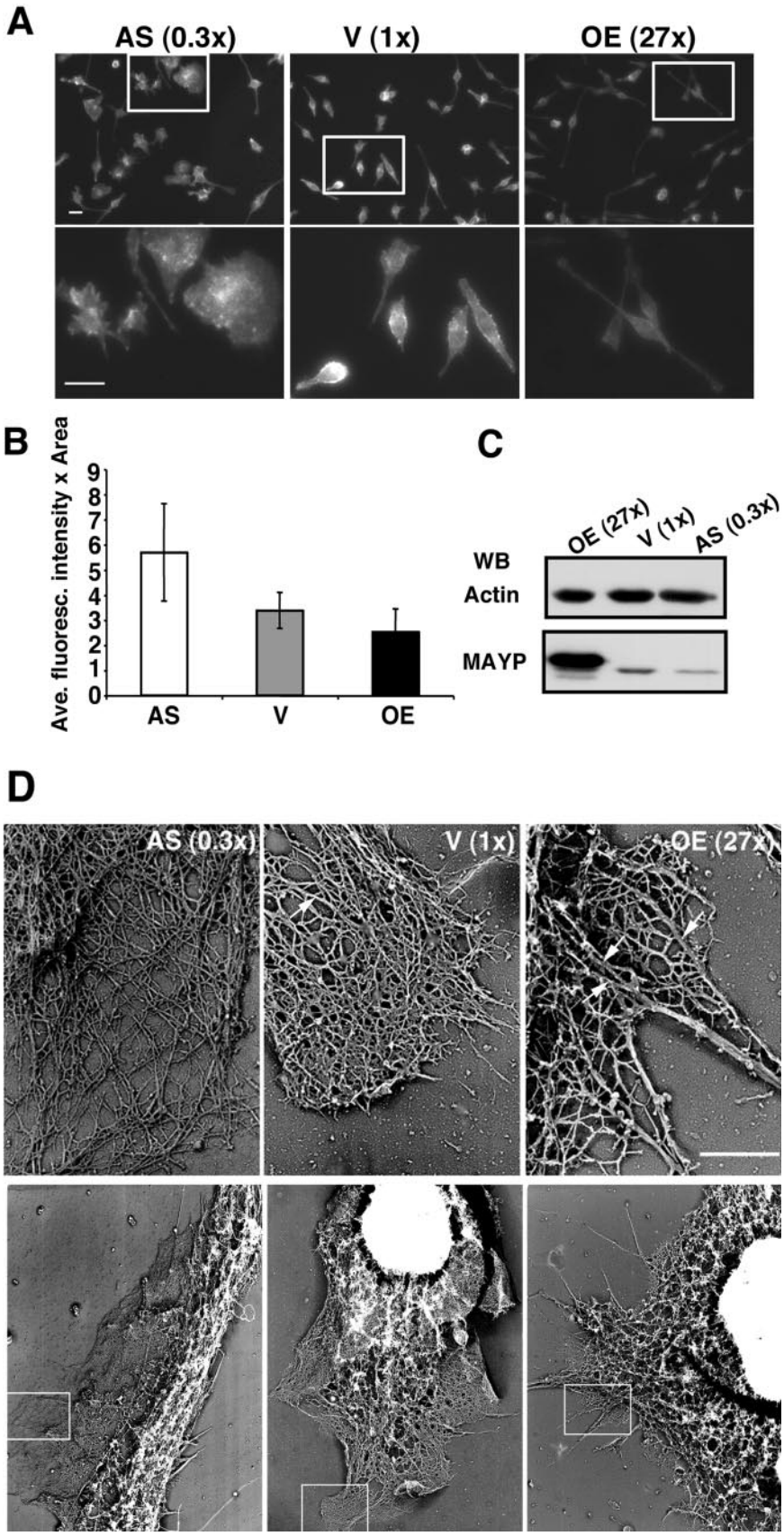

Figure 5. Effects of the level of cellular MAYP expression on F-actin content and microfilament architecture. (A) Cells stained with Rhodamine-labeled Phalloidin. Top, immunofluorescent F-actin staining at 200× magnification; bottom, a 3× magnification of the boxed areas in top panels (Bar, 10 μm). (B) Average fluorescence intensity (±SD) of individual cells in A (≥200 cells/clone) was determined using Image J software. (C) SDS lysates (20 μg/lane) of macrophages of each cell line resolved by SDS-PAGE and Western blotted for actin and MAYP. (D) Transmission electron micrographs of cytoskeletal preparations of cells of each line showing the fine structure of actin filaments in macrophages expressing normal and altered levels of MAYP. Bottom, 4000× magnification; top, boxed areas in the bottom panels, 27,000× magnification. Arrows indicate radially oriented F-actin bundles. Bar, 1 μm.

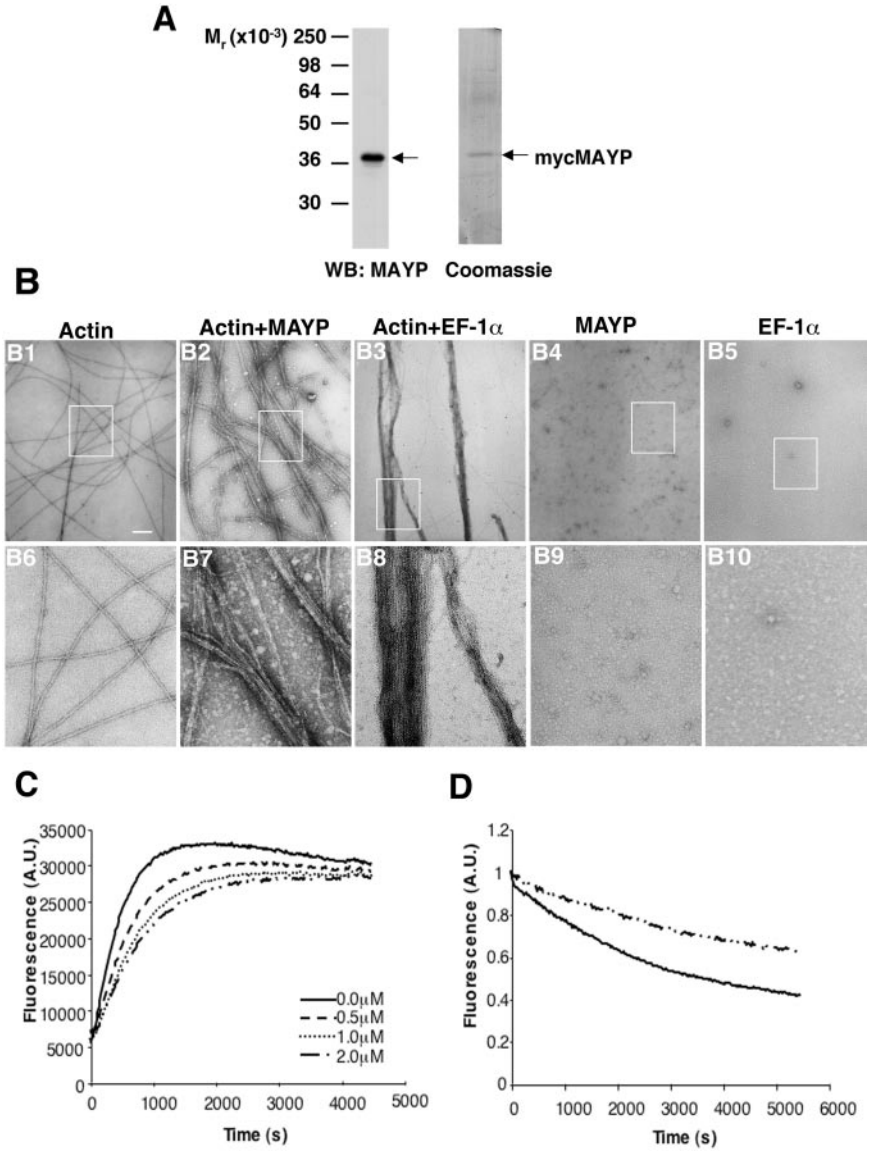

Figure 6. MAYP is an actin-bundling protein. (A) Western Blot of purified myc-tagged MAYP probed with antibodies to MAYP (left) and SDS-PAGE of purified myc-tagged MAYP stained with Coomassie Blue (right). (B) In vitro bundling assay. Actin (3 μM) was polymerized either alone (B1 and B6), with myc-MAYP (1 μM; B2 and B7) or with EF-1α (B3 and B8). Controls include mycMAYP alone (B4 and B9) and EF-1α alone (B5 and B10). The organization of actin fibers was evaluated by electron microscopy at 40,000× magnification. Bottom (B6-B10), a 4× magnification of the boxed areas in the top panels. Scale bar, 200 nm. (C) Actin (3 μM) polymerization in the presence and absence of the indicated concentrations of MAYP. (D) Actin (3 μM) depolymerization in the absence (filled line) and presence (broken line) of MAYP (2 μM).

bundles polymerized with either in vitro using immunogold labeling. Both proteins revealed a similar, uniform distribution along the bundles (Supplementary Figure S4).

MAYP Reduces the Rate of Actin Polymerization In Vitro and Increases F-actin Stability

Macrophages overexpressing MAYP exhibit longer filopodia (Figure 2D). This observation prompted us to determine whether purified MAYP could regulate actin polymerization or F-actin stability. In a pyrene-labeled actin polymerization assay, MAYP reduces the initial rate but not the final extent of actin polymerization in a concentration-dependent manner (Figure 6C). Furthermore, bundled actin filaments obtained by polymerization in the presence of MAYP are more stable to depolymerization than the actin filaments obtained in the absence of MAYP (Figure 6D). Thus, MAYP decreases the rate of actin polymerization in vitro and increases F-actin stability.

Colocalization of MAYP with F-actin In Vivo

To determine where MAYP colocalizes with F-actin in vivo, we performed immunofluorescent staining of MAYP and F-actin. Data supporting the specificity of MAYP staining (primary and secondary antibody controls, immunolocalization of myc-tagged MAYP using anti-MAYP, and anti-myc antibodies) are presented as supplemental material in Supplementary Figure S5. In BAC1.2F5 macrophages, endogenous MAYP was mainly distributed in a punctate manner in the cytoplasm but was also clearly visible lining the cortex (Figure 7, right panel, arrows) and at the bases of filamentous protrusions (Figure 7, right panel, arrowheads) where it colocalized with F-actin (Figure 7, inset).

To determine whether the weak fluorescent signal for MAYP in filopodia indeed represents MAYP associated with actin bundles, we prepared actin cytoskeletons from macrophages and analyzed the location of MAYP using immunogold labeling. Compared with a secondary antibody control (Figure 8A), MAYP distributes in clusters along filamentous projections and at their bases (Figure 8, B and C; Supplementary Figure S6). Clusters of MAYP were also found in the cell cortex (Figure 8, B and D). Similar results were obtained when using anti-myc antibody for detection of myc-tagged MAYP (Supplementary Figure S7).

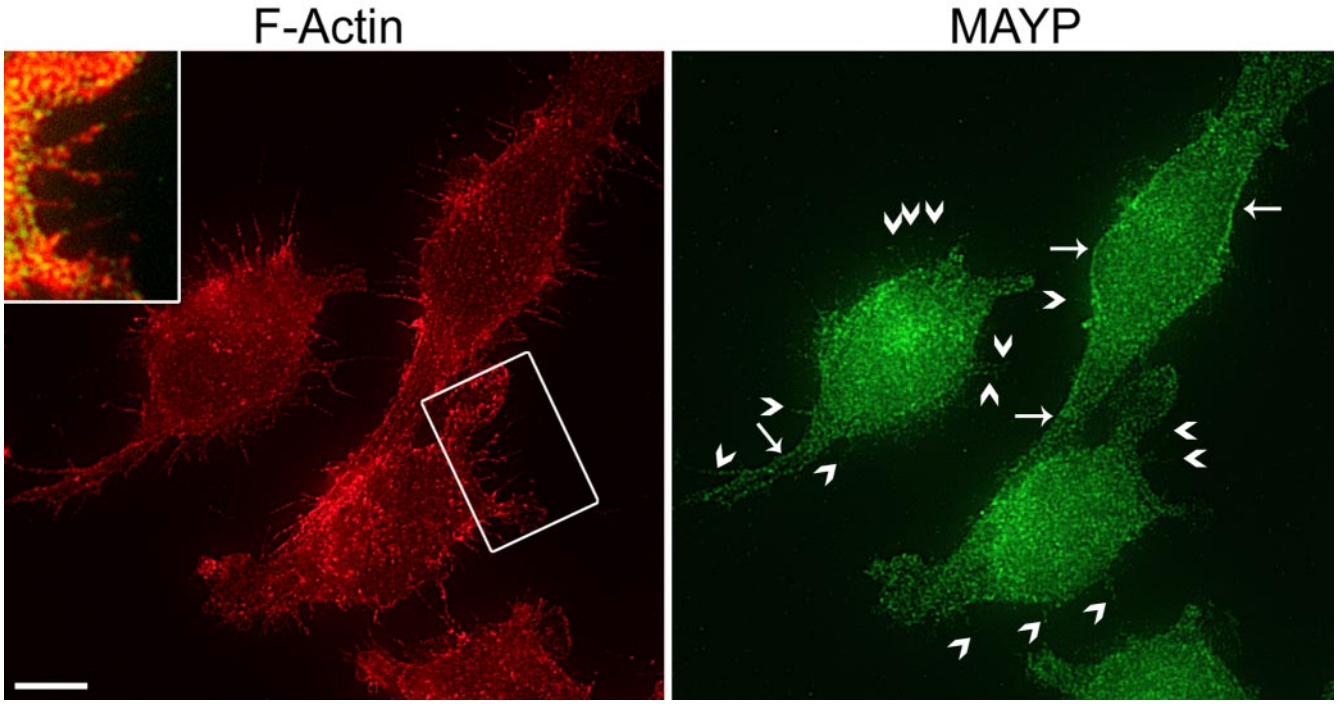

Figure 7. Colocalization of MAYP with F-actin in filopodia. BAC1.2F5 macrophages were grown on fibronectin-coated coverslips, fixed, and stained for F-actin (left) and MAYP (right). Yellow pixels in the insert indicate colocalization. The presence of MAYP at the cell cortex (arrows) and in filopodia (arrowheads) is indicated. Bar, 10 μm.

Thus, consistent with its in vitro actin-bundling activity and in vivo filopodia-inducing activity, MAYP is associated with cortical and filopodial F-actin in vivo.

DISCUSSION

Macrophages are specialized to rapidly change shape, migrate, and phagocytose, and macrophage-specific proteins may contribute to the high degree of flexibility of the macrophage cytoskeleton. We have demonstrated that MAYP/PSTPIP2, a macrophage-specific protein that is tyrosine phosphorylated in response to CSF-1 stimulation (Yeung *et al.*, 1998b), regulates the organization of the actin cytoskeleton to affect morphology and motility. Increased MAYP expression leads to increased actin bundling, filopodia formation, chemokinesis, and chemotaxis, whereas decreased MAYP expression reduces bundling, filopodial numbers, and motility. Moreover, we demonstrate that MAYP controls the pathway connecting CSF-1R tyrosine kinase activation to membrane ruffling because reduced expression of MAYP is associated with increased and prolonged CSF-1–stimulated ruffling, whereas overexpression of MAYP inhibits the CSF-1–stimulated membrane ruffling. The opposite phenotypes of MAYP-overexpressing and -underexpressing macrophages indicate that these changes are specifically attributable to MAYP.

Consistent with MAYP inhibition of CSF-1–induced membrane ruffling, we have shown that MAYP association with F-actin and their colocalization in ruffles is decreased at 1 min of stimulation when MAYP tyrosine phosphorylation and membrane ruffling are increasing. These correlations emphasize the importance of understanding the role of this tyrosine phosphorylation in the regulation of MAYP activity, an area we are currently investigating.

The increased lamellipodial F-actin bundling observed in MAYP-overexpressing cells, focused our attention on MAYP regulation of F-actin bundling. However, despite the association of MAYP with F-actin in vivo (Yeung *et al.*, 1998b), our attempts to demonstrate direct interaction of MAYP with F-actin in vitro using a cosedimentation assay failed, due to the ATP-independent and bivalent cation-dependent oligomerization of MAYP under conditions required for actin polymerization (unpublished data). Therefore, to understand MAYP action in inducing F-actin bundling, we investigated its interaction with actin by examining the morphology of actin filaments polymerized in the presence and absence of purified MAYP. MAYP was found to induce F-actin bundling and to be present on the bundles, demonstrating that it can interact with nascent actin filaments and pack them into bundles in vitro. Unlike some other actin cross-linking proteins, MAYP does not have a pair of identifiable actin-binding domains. However, the coiled coil domain of MAYP (amino acids 93–121) and its adjacent region (amino acids 122–161) are rich in lysine and arginine residues and resemble sequences present in several actin-binding proteins, including paramyosin, myosin heavy chain, villin, and troponin (Yeung *et al.*, 1998b). In addition, MAYP oligomerizes in the presence of bivalent cations (unpublished data), suggesting that the oligomerization of MAYP, in combination with its putative single actin-binding domain, could be important for its actin-cross-linking activity. Further investigations are required to establish the mechanism of interaction between MAYP and actin and the molecular basis for the cross-linking activity of MAYP.

As in the case of another actin-bundling protein, EF-1α (Murray *et al.*, 1997), MAYP was shown to decrease the initial rate of actin polymerization and depolymerization in vitro, but did not affect the final extent of polymerized actin.

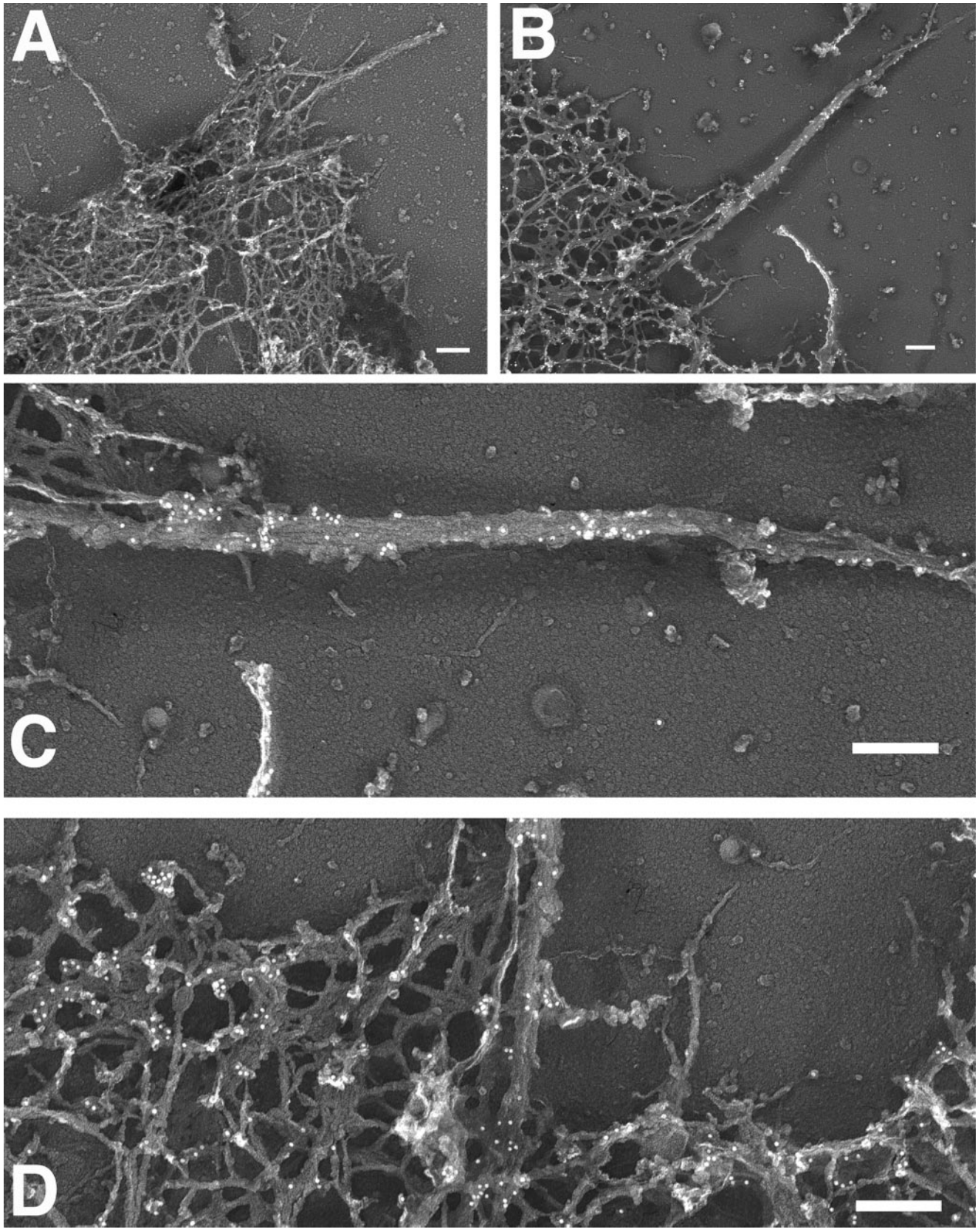

Figure 8. Association of MAYP with the actin cytoskeleton in macrophages. Macrophages overexpressing myc-tagged MAYP were grown on glass coverslips, gently extracted with Triton X-100, fixed and stained with anti-MAYP antibodies and 10-nm gold-conjugated secondary antibodies, rotary shadowed, and examined by transmission electron microscopy at 27,000× magnification. Bar, 200 nm. (A) secondary antibody control; (B–D), MAYP staining.

Assuming that MAYP and EF-1α affect actin polymerization by a similar mechanism, the decrease in actin polymerization rate would be due to the steric blockade of monomer addition to filament barbed ends because the ends become buried in the growing bundle. Purified MAYP does not bind G-actin (unpublished data), therefore its effects on actin polymerization are solely due to its bundling activity. We expect that the increased stability of F-actin polymerized in the presence of MAYP is also due to MAYP-bundling activity because more molecular bonds must be broken to release actin subunits from bundled filaments than from individual filaments.

Interestingly, we found that the bundles obtained with MAYP were less tightly packed and more curved than those produced by EF-1α, suggesting that MAYP participates in the formation of less organized, flexible actin structures.

Actin bundling is important for the formation of filopodia (Svitkina *et al.*, 2003; Vignjevic *et al.*, 2003). Filopodia consist of an unbranched bundle of actin filaments that are aligned axially, with uniform polarity and are packed tightly together by actin bundling proteins (Vignjevic *et al.*, 2003). The roots of filopodia extend well into the actin cortex of the cell where they arise as thin bundles that coalesce into thicker bundles (Svitkina *et al.*, 2003). A convergent elongation model for initiation of filopodia formation has been proposed by Svitkina *et al.* (2003). According to this model, some filaments within the lamellipodial dendritic network acquire privileged status by binding a set of molecules (the tip complex) to their barbed ends which protect them from capping and mediate association of barbed ends with each other on collision. Interestingly, one of the proteins of the tip complex has been shown to be Syndapin I, a PCH family member that causes reorganization of cortical F-actin and formation of filopodia in HeLa cells (Qualmann and Kelly, 2000). As pointed out by Svitkina *et al.* (2003), although Ena/Vasp proteins are responsible for the tip complex prevention of capping, the protein mediating association of barbed ends upon their collision, "the glue molecule," is unknown. The chicken homologue of Syndapin, FAP52, has been shown to aggregate via its coiled coil domains (Nikki *et al.*, 2002), and similarly we have observed (unpublished observations) that MAYP aggregates under actin polymerization conditions. Given the ability of MAYP to bundle actin and to appear in clusters along filopodia, it is conceivable that it functions as a glue molecule in the macrophage. Furthermore, such a function for MAYP is also consistent with its distribution in the cortex of the macrophage, where it is often clustered at the intersection of actin bundles.

Macrophage motility is important in a variety of disease states (Pixley and Stanley, 2004). Of relevance to MAYP, mutations in a closely-related PCH family member, CD2BP1, have been associated with an autoinflammatory disorder known as Pyogenic arthritis pyoderma gangrenosum and acne (PAPA) syndrome (Wise *et al.*, 2002). We have shown that the directional motility and chemotactic response to CSF-1 is proportional to the level of MAYP expression. Filopodia are believed to influence directional motility by acting as environmental sensors (Jones *et al.*, 1998; Bryant, 1999). The MAYP stimulated increase in directional motility and chemotaxis may be partly explained by the increased rate of filopodia formation. However, in addition to sensing the environment, directional cell migration involves repetitive cycles of membrane protrusion, adhesion, de-adhesion, and contraction, processes in which MAYP, a regulator of actin assembly, may well be implicated. Additional studies are required to understand the involvement of MAYP in the regulation of motility and chemotaxis in macrophages.

In conclusion, we have shown that MAYP, a macrophage-specific protein, regulates the morphology and motility of macrophages downstream of the CSF-1R. MAYP inhibits actin reorganization into membrane ruffles and stimulates the formation of filopodia by bundling actin in vitro and in vivo. The coiled-coil region may be important for this function because it contains a putative actin-binding domain and is postulated to mediate the oligomerization of MAYP. Among PCH family members MAYP is unique in that it lacks the SH3 domain, which mediates their interaction with the Wiskott-Aldrich syndrome family of proteins involved in the regulation of actin polymerization. This is the first report of a WASP/N-WASP-independent mechanism of action of a mammalian PCH family protein.

ACKNOWLEDGMENTS

We are grateful to Dr. R. G. Hawley (University of Toronto, Canada) for providing the MSCV-IRES-GFP vector and to Leslie Gunther-Cummins and Michael Cammer (Analytical imaging Facility, Albert Einstein College of Medicine, Bronx, NY) for advice and assistance in the immunogold labeling, collection of time-lapse data, and assistance with the quantitative fluorescence analysis. This work was supported by National Institutes of Health grants RO1 CA 26504 (E.R.S.), PO1 CA 100324 (J.C., E.R.S.), and KO8 CA 097348 (F.J.P.). V.C. is the recipient of a postdoctoral fellowship from the Susan G. Komen Breast Cancer Foundation (PDF0201811).

REFERENCES

Allen, W. E., Zicha, D., Ridley, A. J., and Jones, G. E. (1998). A role for Cdc42 in macrophage chemotaxis. J. Cell Biol. *141*, 1147–1157.

Angers-Loustau, A., Cote, J.-F., Charest, A., Dowbenko, D., Spencer, S., Lasky, L. A., and Tremblay, M. L. (1999). Protein tyrosine phosphatase-PEST regulates focal adhesion disassembly, migration and cytokinesis in fibroblasts. J. Cell Biol. *144*, 1019–1031.

Aspenström, P. (1997). A Cdc42 target protein with homology to the non-kinase domain of FER has a potential role in regulating the actin cytoskeleton. Curr. Biol. *7*, 479–487.

Bailly, M., Macaluso, F., Cammer, M., Chan, A., Segall, J. E., and Condeelis, J. S. (1999). Relationship between Arp2/3 complex and the barbed ends of actin filaments at the leading edge of carcinoma cells after epidermal growth factor stimulation. J. Cell Biol. *145*, 331–345.

Bailly, M., Yan, L., Whitesides, G. M., Condeelis, J. S., and Segall, J. E. (1998). Regulation of protrusion shape and adhesion to the substratum during chemotactic responses of mammalian carcinoma cells. Exp. Cell Res. *241*, 285–299.

Boocock, C. A., Jones, G. E., Stanley, E. R., and Pollard, J. W. (1989). Colony-stimulating factor-1 induces rapid behavioural responses in the mouse macrophage cell line, BAC1.2F5. J. Cell Sci. *93*, 447–456.

Bryant, P. (1999). Filopodia: fickle fingers of cell fate? Curr. Biol. *9*, R655–R657.

Cecchini, M. G., Dominguez, M. G., Mocci, S., Wetterwald, A., Felix, R., Fleisch, H., Chisholm, O., Hofstetter, W., Pollard, J. W., and Stanley, E. R. (1994). Role of colony stimulating factor-1 in the establishment and regulation of tissue macrophages during postnatal development of the mouse. Development *120*, 1357–1372.

Coussens, L. M., and Werb, Z. (2001). Inflammatory cells and cancer: think different! J. Exp. Med. *193*, F23–F26.

Demma, M., Warren, V., Hock, R., Dharmawardhane, S., and Condeelis, J. (1990). Isolation of an abundant 50,000-dalton actin filament bundling protein from *Dictyostelium* amoebae. J. Biol. Chem. *265*, 2286–2291.

DesMarais, V., Ichetovkin, I., Condeelis, J., and Hitchcock-DeGregori, S. E. (2002). Spatial regulation of actin dynamics: a tropomyosin-free, actin-rich compartment at the leading edge. J. Cell Sci. *115*, 4649–4660.

Edmonds, B. T., Wyckoff, J., Yeung, Y.-G., Wang, Y., Stanley, E. R., Jones, J., Segall, J., and Condeelis, J. (1996). Elongation factor-1α is an overexpressed actin binding protein in metastatic rat mammary adenocarcinoma. J. Cell Sci. *109*, 2705–2714.

Ho, H. Y., Rohatgi, R., Lebensohn, A. M., Le, M., Li, J., Gygi, S. P., and Kirschner, M. W. (2004). Toca-1 mediates Cdc42-dependent actin nucleation by activating the N-WASP-WIP complex. Cell *118*, 203–216.

Jones, G., Allen, W., and Ridley, A. (1998). The Rho GTPases in macrophage motility and chemotaxis. Cell Adhes. Commun. *6*, 237–245.

Lewis, C. E., Leek, R., Harris, A., and McGee, J. O. (1995). Cytokine regulation of angiogenesis in breast cancer: the role of tumor-associated macrophages. J. Leukoc. Biol. *57*, 747–751.

Lin, E. Y., Nguyen, A. V., Russell, R. G., and Pollard, J. W. (2001). Colony-stimulating factor 1 promotes progression of mammary tumors to malignancy. J. Exp. Med. *193*, 727–739.

Lippincott, J., and Li, R. (2000). Involvement of PCH family proteins in cytokinesis and actin distribution. Microsc. Res. Tech. *49*, 168–172.

Modregger, J., Ritter, B., Witter, B., Paulsson, M., and Plomann, M. (2000). All three PACSIN isoforms bind to endocytic proteins and inhibit endocytosis. J. Cell Sci. *113*, 4511–4521.

Morgan, C. J., Pollard, J. W., and Stanley, E. R. (1987). Isolation and characterization of a cloned growth factor dependent macrophage cell line, BAC12F5. J. Cell. Physiol. *130*, 420–427.

Muller, A. J., Young, J. C., Pendergast, A. M., Pondel, M., Landau, N. R., Littman, D. R., and Witte, O. (1991). BCR first exon sequences specifically activate the BCR/ABL tyrosine kinase oncogene of Philadelphia chromosome-positive human leukemias. Mol. Cell. Biol. *11*, 1785–1792.

Murray, J. W., Edmonds, B. T., Liu, G., and Condeelis, J. (1997). Elongation factor-1α alters the initial rates and final extent of actin polymerization and depolymerization. J. Cell Biol. *135*, 1309–1321.

Nikki, M., Merilainen, J., and Lehto, V. P. (2002). Focal adhesion protein FAP52 self-associates through a sequence conserved among members of the PCH family of proteins. Biochemistry *41*, 6320–6329.

Persons, D. A., Allay, J. A., Allay, E. R., Ashmun, R. A., Orlic, D., Jane, S. M., Cunningham, J. M., and Nienhuis, A. W. (1999). Enforced expression of the GATA-2 transcription factor blocks normal hematopoiesis. Blood *93*, 488–499.

Pixley, F. J., Lee, P.S.W., Condeelis, J. S., and Stanley, E. R. (2001). Protein tyrosine phosphataseϕ regulates paxillin tyrosine phosphorylation and mediates colony-stimulating-factor 1-induced morphological changes in macrophages. Mol. Cell. Biol. *21*, 1795–1809.

Pixley, F. J., and Stanley, E. R. (2004). CSF-1 regulation of the wandering macrophage: complexity in action. Trends Cell Biol. *14*, 628–638.

Pollard, J. W., and Stanley, E. R. (1996). Pleiotropic roles for CSF-1 in development defined by the mouse mutation osteopetrotic. Adv. Dev. Biochem. *4*, 153–193.

Qualmann, B., and Kelly, R. B. (2000). Syndapin isoforms participate in receptor-mediated endocytosis and actin organization. J. Cell Biol. *148*, 1047–1062.

Rust, W. L., Huff, J. L., and Plopper, G. E. (2000). Screening assay for promigratory/antimigratory compounds. Anal Biochem. *280*, 11–19.

Sherr, C. J., Rettenmier, C. W., Sacca, R., Roussel, M. F., Look, A. T., and Stanley, E. R. (1985). The c-fms proto-oncogene product is related to the receptor for the mononuclear phagocyte growth factor, CSF-1. Cell *41*, 665–676.

Stanley, E. R., Chen, D. M., and Lin, H.-S. (1978). Induction of macrophage production and proliferation by a purified colony stimulating factor. Nature *274*, 168–170.

Stoy, N. (2001). Macrophage biology and pathobiology in the evolution of immune responses: a functional analysis. Pathobiology *69*, 179–211.

Svitkina, T. M., Bulanova, E. A., Chaga, O. Y., Vignjevic, D. M., Kojima, S., Vasiliev, J. M., and Borisy, G. (2003). Mechanism of filopodia initiation by reorganization of a dendritic network. J. Cell Biol. *160*, 409–421.

Takenawa, T., and Miki, H. (2001). WASP and WAVE family proteins: key molecules for rapid rearrangement of cortical actin filaments and cell movement. J. Cell Sci. *114*, 1801–1809.

Tian, L., Nelson, D. L., and Stewart, D. M. (2000). Cdc42-interacting protein 4 mediates binding of the Wiskott-Aldrich syndrome protein to microtubules. J. Biol. Chem. *275*, 7854–7861.

Tushinski, R. J., Oliver, I. T., Guilbert, L. J., Tynan, P. W., Warner, J. R., and Stanley, E. R. (1982). Survival of mononuclear phagocytes depends on a lineage-specific growth factor that the differentiated cells selectively destroy. Cell *28*, 71–81.

Vignjevic, D., Yarar, D., Welch, M. D., Peloquin, J., Svitkina, T., and Borisy, G. (2003). Formation of filopodia-like bundles in vitro from a dendritic network. J. Cell Biol. *160*, 951–962.

Webb, S. E., Pollard, J. W., and Jones, G. E. (1996). Direct observation and quantification of macrophage chemoattraction to the growth factor CSF-1. J. Cell Sci. *109*, 793–803.

Wise, C. A., Gillum, J. D., Seidman, C. E., Lindor, N. M., Veile, R., Bashiardes, S., and Lovett, M. (2002). Mutations in CD2BP1 disrupt binding to PTP PEST and are responsible for PAPA syndrome, an autoinflammatory disorder. Hum. Mol. Genet. *11*, 961–969.

Wu, Y., Dowbenko, D., and Lasky, L. K. (1998a). PSTPIP 2, a second tyrosine phosphorylated, cytoskeletal associated protein that binds a PEST-type protein-tyrosine phosphatase. J. Biol. Chem. *273*, 30487–30496.

Wu, Y., Spencer, S. D., and Lasky, L. A. (1998b). Tyrosine phosphorylation regulates the SH3-mediated binding of the Wiskott-Aldrich syndrome protein to PSTPIP, a cytoskeletal-associated protein. J. Biol. Chem. *273*, 5765–5770.

Wyckoff, J., Wang, W., Lin, E. L., Wang, Y., Pixley, F., Stanley, E. R., Graf, T., Pollard, J. W., Segall, J., and Condeelis, J. (2004). A paracrine loop between tumor cells and macrophages is required for tumor cell migration in mammary tumors. Cancer Res. *64*, 7022–7029.

Yeung, Y.-G., Berg, K. L., Pixley, F. J., Angeletti, R. H., and Stanley, E. R. (1992). Protein tyrosine phosphatase-1C is rapidly phosphorylated in tyrosine in macrophages in response to colony stimulating factor-1. J. Biol. Chem. *267*, 23447–23450.

Yeung, Y.-G., and Stanley, E. R. (1990). Colony stimulating factor-1 receptor. In: Receptor Purification, ed. G. Litwack, Clifton, NJ: Humana Press, 315–328.

Yeung, Y.-G., and Stanley, E. R. (2003). Proteomic approaches to the analysis of early events in colony-stimulating factor-1 signal transduction. Mol. Cell Proteomics *2*, 1143–1155.

Yeung, Y.-G., Wang, Y., Einstein, D. B., Lee, P.S.W., and Stanley, E. R. (1998a). Colony-stimulating factor-1 stimulates the formation of multimeric cytosolic complexes of signaling proteins and cytoskeletal components in macrophages. J. Biol. Chem. *273*, 17128–17137.

Yeung, Y. G., Soldera, S., and Stanley, E. R. (1998b). A novel macrophage actin-associated protein (MAYP) is tyrosine- phosphorylated after colony stimulating factor-1 stimulation. J. Biol. Chem. *273*, 30638–30642.